Electronic Supplementary Information

Nitrogen, sulfur co-doped carbon coated zinc sulfide for efficient hydrogen peroxide electrosynthesis

Chengxiang Dai[a,b], Rongrong Li[a,b], Haichuan Guo[a], Shuqin Liang[a], Hangjia Shen[a*], Tiju Thomas[c*], Minghui Yang[a,b*]

[a]Ningbo Institute of Industrial Technology, Chinese Academy of Sciences, Ningbo, 315201, China

[b]Center of Materials Science and Optoelectronics Engineering, University of Chinese Academy of Sciences, Beijing 100049, China.

[c]Department of Metallurgical and Materials Engineering and the DST Solar Energy Harnessing Center, Indian Institute of Technology Madras, Chennai 600036, India

* Corresponding Author: tt332@cornell.edu; myang@nimte.ac.cn

Experimental edition

Synthesis of ZnS@C

6.39 g sodium diethyldithiocarbamatre(DDTC) and 1.91 g $ZnCl_2$ were dissolved in 150 ml deionized (DI) water using magnetic stirring. The precursor of zinc (II) diethyldithiocarbamate was formed instantly. After stirring for 24 h at room temperature, the white precipitate was separated and wash with DI water and ethanol for several times, and dried at 60 °C for 24 h. Then, it was heated to 700 °C under flowing Ar for 2 h at a heating rate of 5 °C min^{-1}. The sample cooled to room temperature was denoted as ZnS@C. The sample ZnS@C-acid was obtained through the removal of ZnS from ZnS@C in 2 M HCl. 0.2 g ZnS@C was added in a flask with 20 mL 2 M HCl solution in 40 °C for 12 h. The residual sample was collected by the centrifuge (8000 rpm, 2 min) and washed by DI water for three times, and the product was under vacuum at 60 °C for 12 h. Finally, ZnS@C-acid was obtained.

Characterization

Powder X-ray diffraction (PXRD) was performed on MiniFlex 600 X-ray Diffractometer using Cu Kα radiation at a scan rate of 1 ° min-1. X-ray photoelectron spectroscopy (XPS) was collected using an Axis Ultra DLD spectroscope. The morphology was observed on transmission electron microscopy using S4800 and Verios G4 UC field emission scanning electron microscopy (FESEM). Transmission electron microscopy (TEM) and high-resolution transmission electron microscopy (HRTEM) were performed on a Thermo Fisher Talos-F200x TEM with a spherical aberration corrector. The element distribution of composites wasdetermined with an energy dispersive spectrometer (EDS) attached to the TEM instrument.

Electrochemical measurements

A three–electrode system was measured on CHI 760E to collect electrochemical measurements at room temperature. A saturated calomel electrode (SCE) and a graphite electrode were as the reference and counter electrode. All the potentials were calibrated to the reversible hydrogen electrode (RHE) using the equation:

$$E_{RHE} = E_{SCE} + (0.273 + 0.0592pH)V \quad (1)$$

The catalyst ink was prepared by mixing NC-900 in isopropanol/water solution =1:1 with Nafion ionomer (0.1%). After sonication for 30 min, catalyst ink was loaded onto a glassy carbon electrode (d=5.61 cm) with a catalyst loading of 0.3 mg cm^{-2}. Linear sweep voltammetry (LSV) curves were carried out in 0.1 M KOH solution at a rotation speed of 1600 rpm. Polarization curves in Ar-saturated electrolytes were recorded as background current at a scan rate of 10 mV s^{-1}. The Pt ring was set at a constant potential of 1.15 V (*vs.* RHE) during all tests.

Gradual degradation of I_r was collected during the continuous rotating ring-disk electrode (RRDE) stability test, which according to the previous literature can be readily recovered by rapid cyclic voltammetry at low potentials to reduce PtOx.[1] The H_2O_2 selectivity and the number of electrons transferred are calculated based on the followed equations consisted of both disk and ring currents:

$$H_2O_2 \text{ selectivity } (\%) = 200 \times (I_r/N)/(I_d + I_r/N) \quad (2)$$

$$n = 4 \times I_d/(I_d + I_r/N) \quad (3)$$

where I_d is the disk current, I_r is the ring current, N is the current collection efficiency. As previous literature,[2] N was measured in the ferrocyanide/ferricyanide half reaction system at the rotation rate of 1600 rpm.

For peroxide reduction reaction (PRR) analysis, the polarization curves were recorded at the rotation rate of 1600 rpm in Ar-saturated 0.1 M KOH with 10 mM H_2O_2.

Electrocatalytic H_2O_2 production in 0.1 M KOH was performed in a two-chamber cell with Nafion 115 membrane as the separator. Both the cathode compartment (17 ml) and anode compartment were filled with the same electrolyte (0.1 M KOH). The working electrode was prepared by coating of the catalyst ink on

the carbon paper (CP, the efficient area is 0.785 cm^2) with a catalyst loading of 0.3 mg cm^{-2}.

H_2O_2 concentration was determined using H_2O_2 electroanalysis method using a platinum sheet as working electrode. CHI 760E workstation was applied in analytical testes. This method is based on different response currents of changed H_2O_2 concentrations in 0.1 M KOH. Chronoamperometry was used to measure currents at applied potential of 1.15 V (*vs.* RHE). In order to draw a calibration curve, we measured the current with the addition of different standard H_2O_2 solution. Based on the linear fitting of H_2O_2 concentration with the response current, the H_2O_2 concentration produced can be determined.

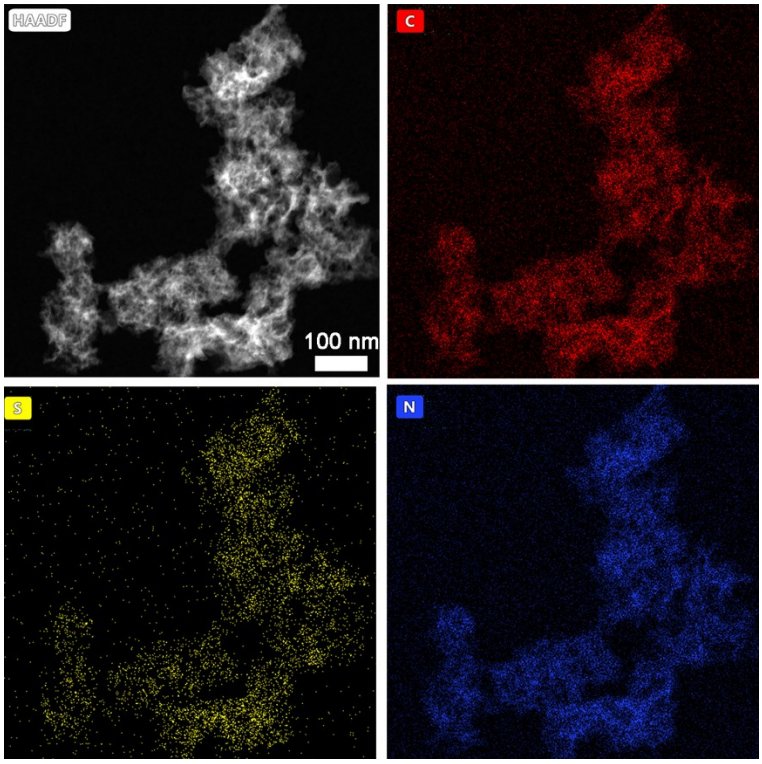

Figure S1. HAADF-STEM and EDX mapping images of C, N, S (ZnS@C-acid).

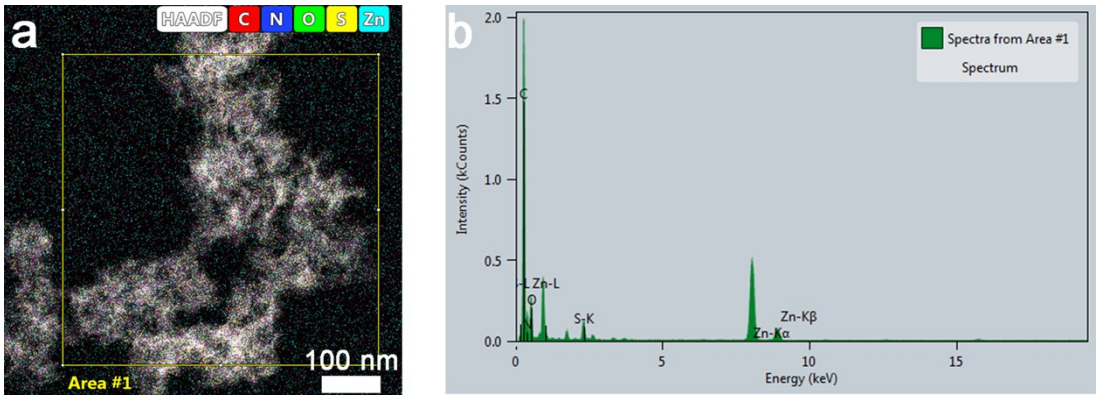

Figure S2. HAADFSTEM and EDX mapping images of C, N, S, Zn (ZnS@C-acid) (a) and the analysis of elementary distribution of ZnS@C-acid (b).

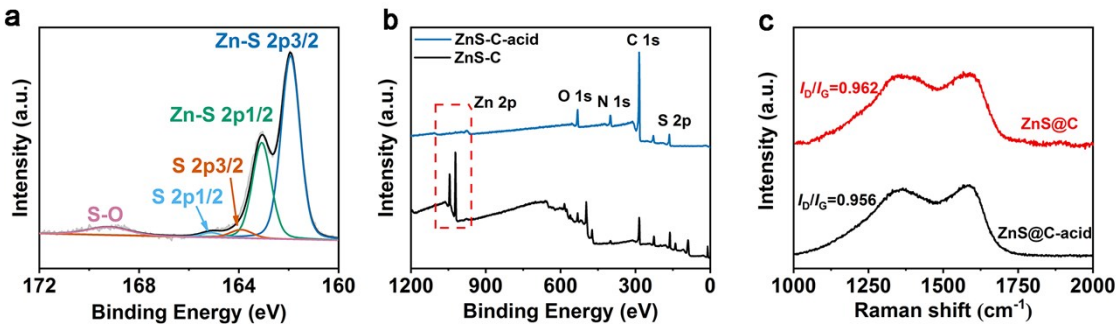

Figure S3. (a) The detailed deconvoluted S 2p survey of ZnS@C. (b) Fully scanned XPS spectra of the surface chemical composition of ZnS@C and ZnS@C-acid. (c) Raman spectra of ZnS@C and ZnS@C-acid.

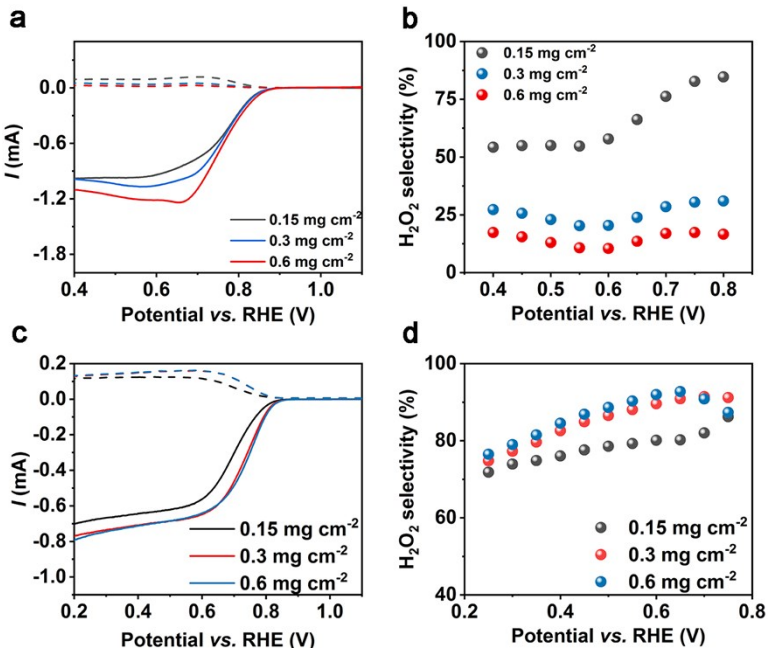

Figure S4. Polarization curve and real-time ring current of ZnS@C-acid (a) and ZnS@C (c) at different loading amount. The corresponding H_2O_2 selectivity of ZnS@C-acid (b) and ZnS@C (d).

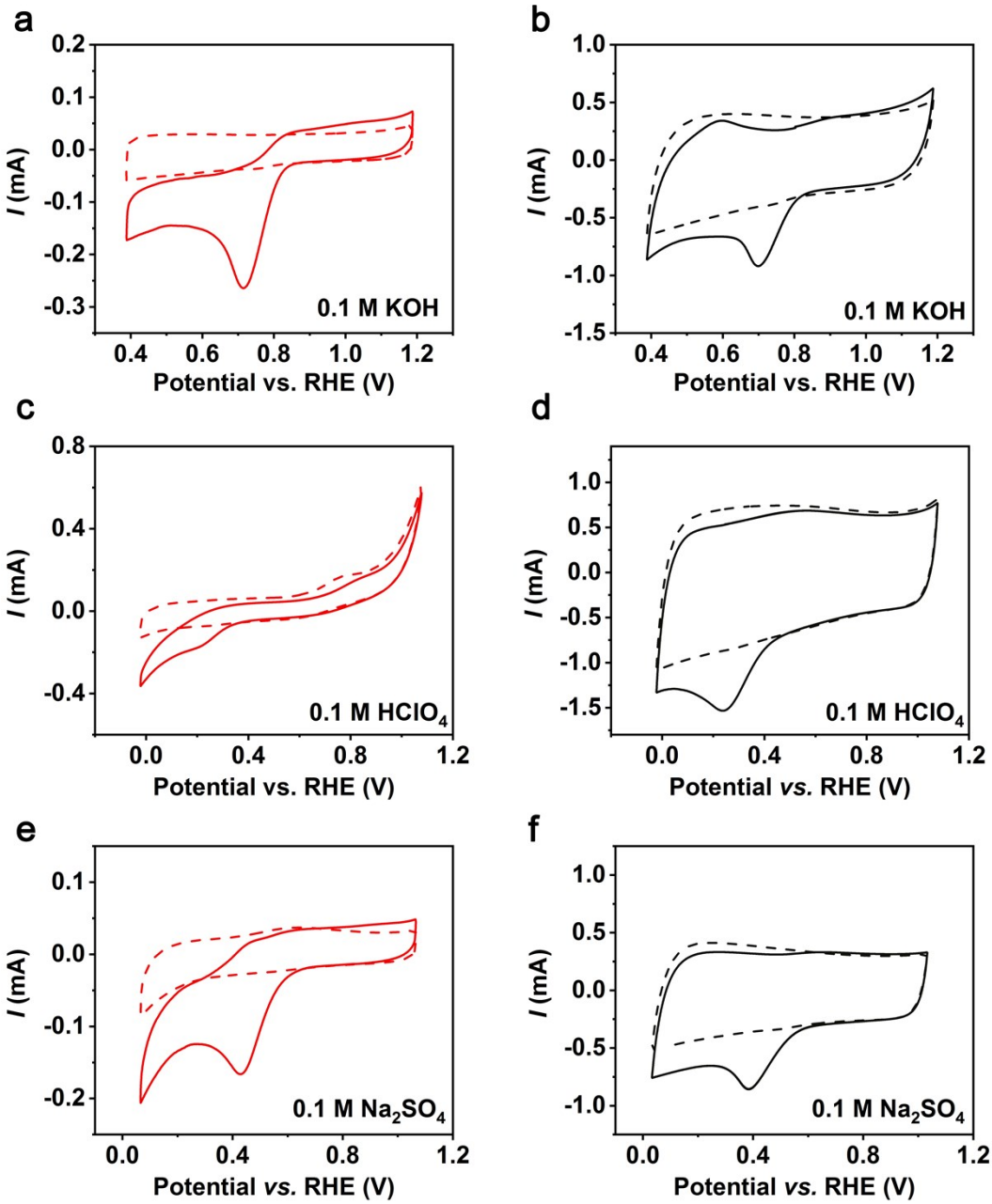

Figure S5. CV tests of ZnS@C (a, c, e) and ZnS@C-acid (b, d, f) in O_2-saturated (solid line) and Ar-saturated (dash line) electrolyte.

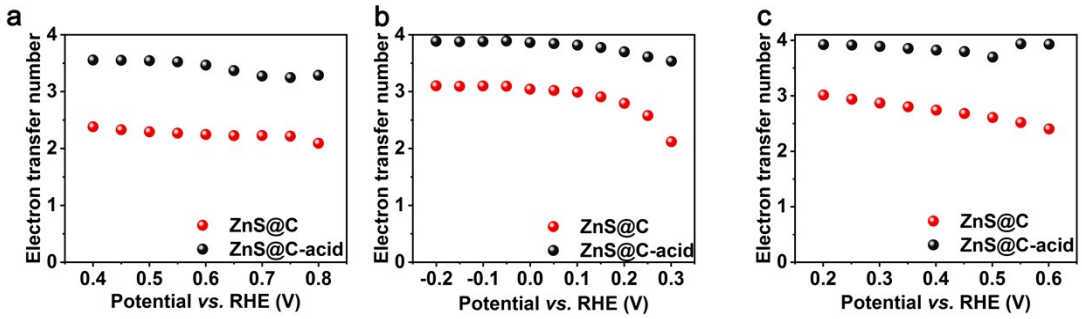

Figure S6. Electron transfer number of ZnS@C and ZnS@C-acid in 0.1 M KOH (a), 0.1 M $HClO_4$(b) and 0.1 M Na_2SO_4(c).

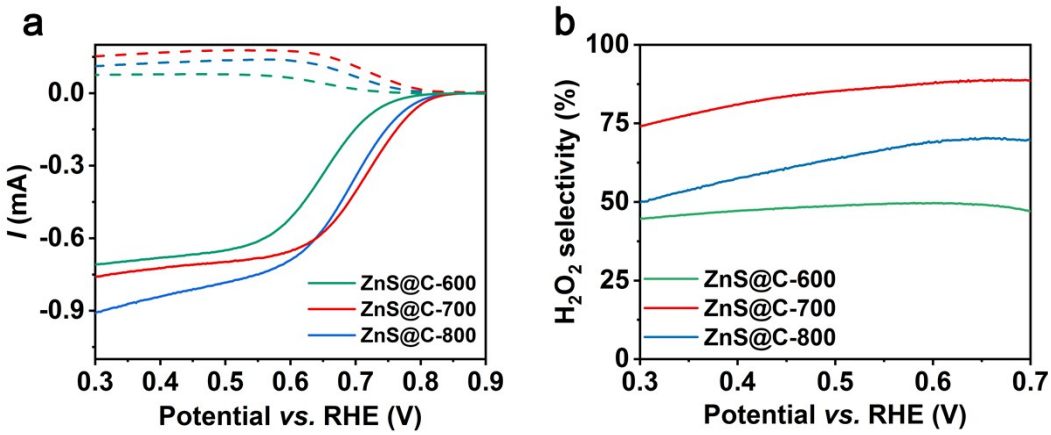

Figure S7. LSV (solid lines) of RRDE with the ring current (dashed lines) collected on the Pt ring at 1600 rpm in the O_2-saturated 0.1 M KOH.

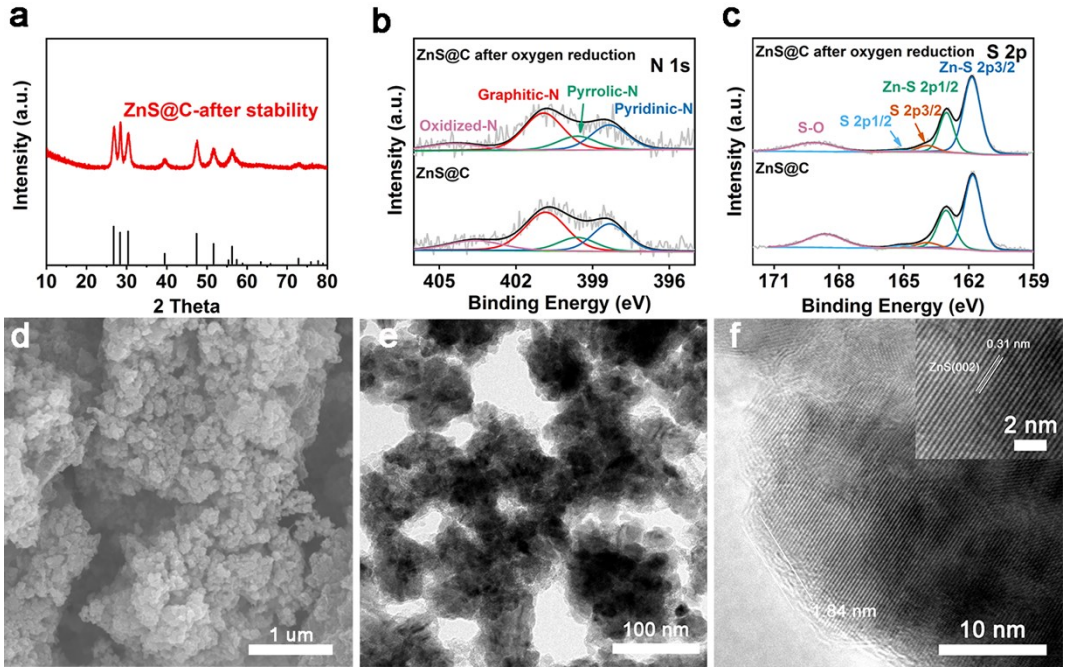

Figure S8. (a) PXRD of ZnS@C after long-term oxygen reduction. (b) High-resolution XPS N 1s spectrum of ZnS@C before and after long-term oxygen reduction. (c) High-resolution XPS S 2p spectrum of ZnS@C before and after long-term oxygen reduction. (d) SEM images of ZnS@C after oxygen reduction. (e) TEM of ZnS@C after oxygen reduction.

Table S1. The content of elementary in the ZnS@C-acid by TEM.

Element Family	Mass Fraction (%)	Mass Error (%)	Fit Error (%)
C	84.19	3.72	3.02
N	2.53	0.60	12.63
O	8.43	1.71	0.96
S	4.57	0.86	0.69
Zn	0.28	0.05	8.85

Table S2. Reactivity and selectivity comparison of the N, S co-doped carbon coated zinc sulfide and other reported electrocatalysts for H_2O_2 through ORR that involves $2e^-$ process.

Sample	Loading (mg cm^{-2})	Potential @ 1 mA cm^{-2}(V vs.RHE)	Selectivity @ 1.0 mA cm^{-2}	Electrolyte	Ref.
N-O-P-C-800	0.19	0.59	90%	0.1 M KOH	[3]
NCA-850	0.196	0.7	90%	0.1 M KOH	[4]
CB-600	0.2	0.74	52.6%	0.1 M Na_2SO_4	[5]
Fe-CNT	0.1	0.76	90%	0.1 M KOH	[1]
O-CNT	0.1	0.7	90%	0.1 M PBS	[6]
Co-POC-O	0.1	0.78	84%	0.1 M KOH	[7]
cCNT	0.6	0.6	~85%	0.1 M KOH	[8]
FRC	0.2	0.62	~95%	0.1 M KOH	[9]
G250	0.255	0.39	~75%	0.1 M KOH	[10]
meso-BMP-800	0.3	0.33	~65%	0.1 M $HClO_4$	[11]
CB+CTAB	0.24	0.71	~95%	0.1 M KOH	[12]
ZnS@C	0.3	0.74	88.9%	0.1 M KOH	this work

Reference

1. K. Jiang, S. Back, A. J. Akey, C. Xia, Y. Hu, W. Liang, D. Schaak, E. Stavitski, J. K. Norskov, S. Siahrostami and H. Wang, *Nat Commun*, 2019, **10**, 3997.
2. R. Zhou, Y. Zheng, M. Jaroniec and S.-Z. Qiao, *ACS Catalysis*, 2016, **6**, 4720-4728.
3. H.-X. Zhang, S.-C. Yang, Y.-L. Wang, J.-C. Xi, J.-C. Huang, J.-F. Li, P. Chen and R. Jia, *Electrochimica Acta*, 2019, **308**, 74-82.
4. H. Zhao, X. Shen, Y. Chen, S. N. Zhang, P. Gao, X. Zhen, X. H. Li and G. Zhao, *Chem Commun (Camb)*, 2019, **55**, 6173-6176.
5. H. Zhang, Y. Li, Y. Zhao, G. Li and F. Zhang, *ACS Appl Mater Interfaces*, 2019, **11**, 27846-27853.
6. Z. Lu, G. Chen, S. Siahrostami, Z. Chen, K. Liu, J. Xie, L. Liao, T. Wu, D. Lin, Y. Liu, T. F. Jaramillo, J. K. Nørskov and Y. Cui, *Nature Catalysis*, 2018, **1**, 156-162.
7. B. Q. Li, C. X. Zhao, J. N. Liu and Q. Zhang, *Adv Mater*, 2019, **31**, e1808173.
8. L. Z. Peng, P. Liu, Q. Q. Cheng, W. J. Hu, Y. A. Liu, J. S. Li, B. Jiang, X. S. Jia, H. Yang and K. Wen, *Chem Commun (Camb)*, 2018, **54**, 4433-4436.
9. Z. Meng, J. Li, F. Huo, Y. Huang and Z. Xiang, *Chemical Engineering Science*, 2017, **174**, 222-228.
10. C. Y. Chen, C. Tang, H. F. Wang, C. M. Chen, X. Zhang, X. Huang and Q. Zhang, *ChemSusChem*, 2016, **9**, 1194-1199.
11. T. P. Fellinger, F. Hasche, P. Strasser and M. Antonietti, *J Am Chem Soc*, 2012, **134**, 4072-4075.
12. K.-H. Wu, D. Wang, X. Lu, X. Zhang, Z. Xie, Y. Liu, B.-J. Su, J.-M. Chen, D.-S. Su, W. Qi and S. Guo, *Chem*, 2020, **6**, 1443-1458.